Celal Bayar University Journal of Science

The Effect of Substrate Dielectric Constant and Thickness on Millimeter Wave Band Patch Antenna Performance

Seda Ermis[1]*

[1] Osmaniye Korkut Ata University, Electrical and Electronics Engineering Department, Osmaniye, Türkiye
*sedaermis@osmaniye.edu.tr
* Orcid No: 0000-0002-3105-7080

Abstract

In last decade, the fifth generation of telecom network (5G) has been a new era as a result of fast-growing mobile industry. Unlike its predecessors, 5G will not only provide faster, better mobile broadband experience, but also broaden communication network with new services such as device-to-device communications or connecting IoT devices and users. For this purpose, 5G aims to achieve massive network capacity, ultra-low latency, higher data speed and greater network reliability. According to the report of ITU World Radiocommunication Conference 2019 (WRC-19), several new frequency bands between 20-70 GHz, were announced for allocation of 5G. Frequencies in the Ka-band (27-40 GHz) are particularly attractive due to their low atmospheric attenuation. At the specified frequency range i.e., millimeter wave band, antenna design for 5G applications is very crucial to provide high gain and efficiency as well as broadband communication which is indispensable for high-speed data traffic. At this point, Microstrip patch antennas, stand out amongst others because of their numerous attractive features. In this work, the effect of substrate dielectric constant and thickness to the Rectangular Microstrip Antenna (RMA) performance is examined for high frequency 5G applications. The RMA is designed to operate at 38 GHz and antenna performance has been analyzed according to various dielectric substrates, such as RT5880, RO3003, FR4, RT6006 and RT6010, considering different dielectric constants, thicknesses, and tangential losses. All designs and analyses have been accomplished by using ANSYS HFSS (High-Frequency Structure Simulator) and comparative results of the work are presented.

Keywords: 5G, 38 GHz, RMA, Substrate Dielectric Constant, Substrate Thickness

1. Introduction

In 2011, the evolution of 4G/LTE wireless technology has been pivotal to offer much higher data rate and reduced latency for mission critical applications, thereby expanding wireless network capacity with more advanced multimedia services. Following the global deployment of 4G/LTE networks, the increasing number of mobile phone users and multimedia applications led to a significant rise in mobile traffic. According to Cisco, mobile traffic experienced approximately 70% growth in 2014 and 63% growth in 2016. [1-3].

As the upcoming generation over 4G, The Fifth Generation of Mobile Technology, or 5G, aimed not only provide a peer-to-peer mobile communication but also a connection between users and IoT devices which means massive growth of mobile data in its various forms. For

this purpose, major requirements for 5G were defined as follows [3,4];

- Ten times higher data rate (1~10 Gbps) from traditional 4G/LTE network's peak data rate of 150 Mbps
- Around 1 ms round trip latency which indicates almost ten times reduced latency from 4G's 10 ms round trip time
- Wide bandwidth to enable many linked devices to use for longer periods of time in one location
- Offer connectivity to thousands of devices in order to realize the IoT goal
- 99.999% Perceived availability and guarantee full coverage regardless of users' location
- Long battery life and decrease in energy consumption

To meet these requirements, 4G wireless communications spectrum which is between 300 MHz and 3 GHz band was expanded with high frequency

millimeter wave (mm-wave) band, ranging from 3∼300 GHz. Thus, even a small fraction of the available mm-wave spectrum has the potential to provide data rates and capacity that are hundreds of times higher than those offered by the existing cellular spectrum [5].

5G was defined in 2018 by the 3rd Generation Partnership Project (3GPP). In addition to frequencies below 6 GHz (3.3-3.8 GHz), which are similar to existing 4G frequencies in the transition from 4G LTE to 5G, an additional spectrum area, called the millimeter band, has been opened in the 20-70 GHz range [4-6]. Frequencies within the Ka-band (27-40 GHz) are particularly noteworthy due to their low atmospheric attenuation. Despite these advancements, 5G technology has not yet been fully deployed, and ongoing research efforts aim to further its development [7-11].

Although 5G features such as high data rate and minimum latency can be achieved relatively easily, signal path loss, multipath effect, connection losses, short-scale signal attenuation and narrow network coverage are still problems for this communication technology. Ongoing studies to improve 5G system performance includes creating radiation in the desired form, improving antenna impedance bandwidth, using narrow beam width and high gain antenna, small cell technology and MIMO (Multiple Input Multiple Output) antenna with high beam directing feature and low scanning loss etc. To overcome these problems and improve 5G network performance develop an efficient antenna design has great importance [12-13].

For a reliable signal transmission in mobile communication, it is desired to use a small size, high gain, low loss, high performance broadband antenna. Traditionally, Microstrip Patch Antennas are the most popular candidate for 5G applications, which are frequently preferred by many researchers because of low cost, light weight, ease of manufacture and installation, durability, and easy integration into microwave circuits. However, besides these advantages, microstrip antennas also have narrow bandwidth, limited gain and low efficiency. To address these issues, researchers have explored various techniques to enhance the gain and bandwidth of patch antennas and improve their performance. Some of the widely recognized and frequently utilized methods are adding parasitic patch element to the antenna structure, slotting on the patch surface, defecting ground surface (DGS), the increment of substrate thickness, use of coupling type of feeding and the design of array configurations. These methods are well-documented in the literature [5,14-24].

For instance, Demirci employed non-contacting insert feeding and proximity coupling feeding techniques to design both single and array-type rectangular microstrip antennas that resonate at 28 GHz, in 2020 [5].

Additionally, the introduction of slits on the surface of the upper patch enabled dual-band operation at 28 GHz and 38 GHz [15]. Furthermore, it was reported that the antenna gain increased with the use of 2-element and 4-element Rectangular Microstrip Antenna (RMA) array designs. Also, the bandwidth of the antenna improved through the use of defected ground structures or by incorporating parasitic patch into the design [22].

In 2020, Sharaf et al. introduced a compact dual-frequency microstrip patch antenna designed for dual-band 5G applications operating at 38 and 60 GHz. The proposed antenna consisted of two electromagnetically coupled patches printed on the Rogers RO3003 substrate with the dielectric constant (ε_r) of 3, a loss tangent (δ) of 0.001 and a thickness (h) of 0.25 mm. Experimental results revealed that the impedance matching bandwidths (for $|S_{11}| < -10dB$) and gains were approximately 2 GHz and 6.5 dBi for the 38 GHz band, and 3.2GHz and 5.5 dBi for the 60 GHz band, respectively [14].

In 2020, Haneef et al. conducted a performance analysis of a rectangular microstrip antenna operating at 28 GHz using various dielectric substrates. In their study, the substrate thickness was maintained at 1.6 mm, and the evaluation focused exclusively on antenna gain. However, for 5G applications, wide bandwidth is a crucial parameter for enabling higher data transfer rate, which was not considered in the analysis. The study identified RT-Duroid 6010 as the most suitable substrate for 5G applications, featuring a thickness of 1.6 mm, a loss tangent of 0.0023, and a dielectric constant of 10.2. Besides the limitation of very narrow bandwidth, another drawback of this study was that the use of a thick substrate with a high dielectric constant increases surface current, which can lead to higher-order wave modes, high degree of side/back lobe level and multiple resonance frequencies. These issues are particularly significant for MIMO antenna arrays, as it may result in mutual coupling, electromagnetic interference, and crosstalk effects [16].

Similarly, in 2020, Ramli et al. presented an analysis of a 3.5 GHz microstrip patch antenna design utilizing three different substrate materials: FR-4, RT-5880, and TLC-30, with respective thicknesses of 1.6 mm, 1.575 mm, and 1.58 mm. The reported gains for the antenna were 3.338 dB for FR-4, 4.660 dB for RT-5880, and 5.083 dB for TLC-30. Additionally, the bandwidths observed for these substrates were 247.1 MHz for FR-4, 129.7 MHz for RT-5880, and 177.2 MHz for TLC-30 [17].

Sree et al., in 2021, designed and fabricated a microstrip patch antenna for sub-6 GHz band 5G applications. The proposed antenna was based on Rogers RO5880 substrate with a dielectric constant of 2.2 and a thickness of 1.6 mm. To achieve dual-band operation, the Defected Ground Structure (DGS) technique was applied to the patch layer. Experimental results demonstrated overall

gains of 5 dB and 4.57 dB at 4.53 GHz and 4.97 GHz, respectively. However, the study did not investigate the effect of varying substrate thickness on antenna performance. It is generally understood that reducing the substrate thickness can enhance gain due to lower associated losses [19].

In 2023, Kumar et al. proposed a compact, tri-band, slotted monopole antenna with a hexagonal shape patch for sub-6 GHz of 5G applications such as Wi-Fi, WLAN or WiMAX. In the designed and manufactured antenna, 1.6 mm thick FR-4 substrate was used and DGS technique was applied to increase bandwidth. The measured peak gains were 1.35 dB at 2.45 GHz, 2.55 dB at 3.65 GHz and 3.8 dB at 5.5 GHz. Also, measured bandwidths were reported as 112 MHz, 700 MHz and 1359 MHz at 2.45 GHz, 3.65GHz and 5.5 GHz respectively [23].

Numerous examples of microstrip patch antenna designs are documented in the literature, encompassing a wide range of frequency bands, patch geometries, substrate types, and thicknesses. Additionally, various performance enhancement techniques have been applied to these antennas, and this review could be expanded to include these examples. Regardless of the method employed, researchers generally begin by defining the antenna geometry, operating frequency, substrate permittivity, and thickness as the initial steps in their design process. Due to the absence of analytical methods for calculating the propagation characteristics of microstrip antennas with arbitrarily shaped patches, the desired operational frequency range is typically determined through parametric studies and optimization of antenna dimensions, with the aid of specialized software. When selecting the dielectric constant and thickness of the substrate, antenna engineers must thoroughly understand and assess their impact on antenna performance within the specific frequency band of interest. Such an understanding will facilitate more accurate predictions for complex antenna design studies and lead to more successful outcomes through appropriate substrate selection. Furthermore, the literature indicates a gap in comprehensive evaluations, particularly concerning how substrate characteristics affect antenna performance in the millimeter-wave band, highlighting an area that merits further investigation.

For these reasons, in this study, the effect of substrate dielectric constant and thickness to the Rectangular Microstrip Antenna (RMA) performance is examined for high frequency 5G applications. The RMA is designed to operate at 38 GHz due to low atmospheric attenuation at Ka-band. Then, antenna performance has been analyzed according to various dielectric substrates, such as RT5880, RO3003, FR4, RT6006 and RT6010 as well as dielectric constants, thicknesses and tangential loss. All designs and analyses have been accomplished by using

ANSYS HFSS (High-Frequency Structure Simulator) and comparative results of the work are presented.

2. Materials and Methods

The most commonly used microstrip antennas have shape of rectangular. The basic form of a Rectangular Microstrip Antenna (RMA) consists of a ground plane, a dielectric substrate and a patch with feed line. As seen from the Fig.1, width and length of the radiating patch are W_p and L_p, whereas W_g and L_g are width and length of the ground plane, ε_r is the dielectric constant of the substrate, h and t are thicknesses of the dielectric and patch, respectively.
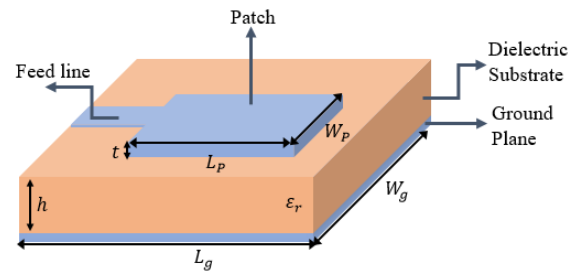

Figure 1. Geometry of the RMA

Many different dielectric materials can be used in design microstrip antennas and generally, their dielectric constants are in the range of $2.2 \leq \varepsilon_r \leq 12$ with the thickness $h \ll \lambda_0$ (λ_0 is the free space wavelength). For enhanced antenna efficiency, wider bandwidth, and a more loosely bound radiation field, thick substrates with lower dielectric constants are generally preferred. However, this approach results in increased antenna size and can lead to less stable radiation patterns. Conversely, thin substrates with high dielectric constants are favored for microstrip antennas integrated into microwave circuits. Such substrates confine the radiation more effectively to the substrate, leading to more stable radiation and minimizing unwanted radiation areas. Nevertheless, this choice tends to increase loss and reduce bandwidth [25].

The dimensions of a rectangular patch antenna can be mathematically calculated using straightforward formulas derived from the transmission line model or cavity model. These approaches offer designers a simple and efficient means to estimate the antenna dimensions required for a specific resonance frequency and they are most accurate for thin substrates at lower frequencies. In the transmission line model, the design procedure begins by determining the substrate dielectric constant (ε_r), substrate thickness (h) and resonance frequency (f_r). For an efficient radiator, a practical patch width W_p that leads to good radiation efficiencies is

$$W_p = \frac{1}{2f_r\sqrt{\mu_o\varepsilon_o}}\sqrt{\frac{2}{\varepsilon_r + 1}} = \frac{\vartheta_o}{2f_r}\sqrt{\frac{2}{\varepsilon_r + 1}} \qquad (1)$$

where $\vartheta_O = c = 3 \times 10^8 \; m/sn$, $\mu_o = 4\pi \times 10^{-7} \; H/m$, $\varepsilon_o = 8.85 \times 10^{-12} \; F/m$ are speed of light, magnetic permeability and dielectric constant in free space respectively. Due to the finite dimension of the patch, radiation occurs at the edges of the patch and it can be represented by two radiating slots along the length. Although electric field lines mostly concentrate in the substrate, some part of it is placed in the air due to the fringing effect [25]. Therefore, nonhomogeneous line of two dielectrics is taken into account by calculation of the effective dielectric constant which is given as,

$$\varepsilon_{reff} = \frac{\varepsilon_r + 1}{2} + \frac{\varepsilon_r - 1}{2}\left[1 + 12\frac{h}{W_p}\right]^{-\frac{1}{2}}$$
$$where \quad \frac{W_p}{h} > 1 \qquad (2)$$

At lower frequencies the ε_{reff} remains relatively constant, often referred to as a static value. However, as the operating frequency increases, particularly in the millimeter wave band, ε_{reff} approaches the dielectric constant of the substrate. Therefore, ε_{reff} is, in fact, a frequency-dependent parameter [25]. On the other hand, due to the fringing effect, the patch looks greater electrically than its physical dimension. and so, the increment in length ΔL and the effective length of the patch are calculated as;

$$\Delta L = \frac{0.412h(\varepsilon_{reff} + 0.3)\left(\frac{W_p}{h} + 0.264\right)}{(\varepsilon_{reff} - 0.258)\left(\frac{W_p}{h} + 0.8\right)} \qquad (3)$$

$$L_{eff} = \frac{1}{2f_r\sqrt{\varepsilon_{reff}}\sqrt{\mu_o \varepsilon_o}} \qquad (4)$$

Therefore, the actual length of the patch, L_p, is

$$L_p = L_{eff} - 2\Delta L = \frac{1}{2f_r\sqrt{\varepsilon_{reff}}\sqrt{\mu_0 \varepsilon_o}} - 2\Delta L \qquad (5)$$

The theoretical calculations for antenna and microstrip line impedances are detailed in Ref. [25]. While the transmission line model is effective for practical calculations of rectangular patch dimensions at lower frequencies for thin substrates, it has limitations. To address these limitations and achieve more accurate results, particularly for designs beyond these constraints, it is necessary to employ simulation software to optimize antenna dimensions and obtain precise performance predictions.

In this study, single RMA is designed to operate 38 GHz and antenna performance has been analyzed according to various dielectric substrates and thicknesses using ANSYS HFSS software, as explained in the following section.

2.1 38 GHz Single RMA Design and Analyses

A single RMA operates at 38 GHz was designed by HFSS simulation environment. The antenna structure comprises a concentric upper patch, a bottom patch (ground plane) and a substrate, with the center of the antenna structure aligned at the origin. Antenna is fed by 50Ω non-contact inset-feed to enhance key performance parameters such as gain, bandwidth, efficiency, return loss and directivity. The dimensions of both antenna and feed line were optimized for impedance matching and maximum power transfer. Fig. 2 illustrates the top view of the RMA geometry and in Fig.3, its simulated 3D model in the HFSS software is depicted.
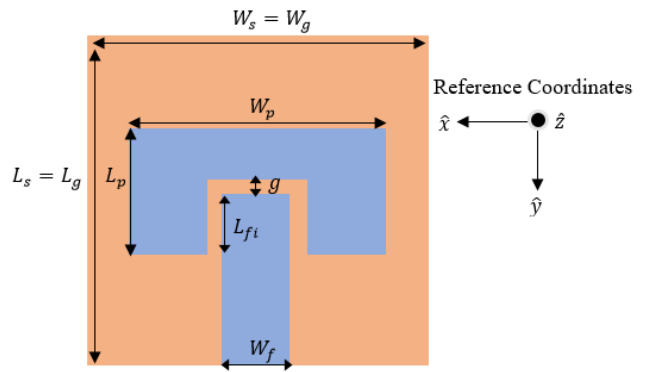

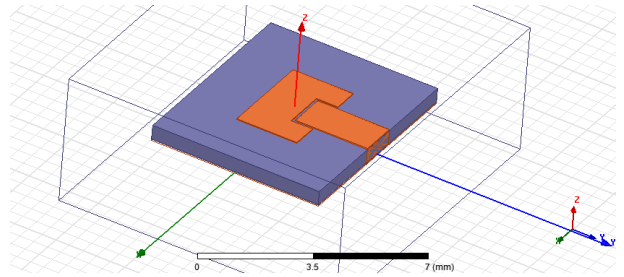**Figure 2.** Top view of the designed RMA geometry

Figure 3. Constructed 3D RMA geometry in the simulation environment

Due to gap (g) between patch and feed line, energy is provided by coupling effect and this feeding technique allows to optimize patch and feed line separately. Hence, the gap (g) between patch and feed line, as well as dimensions of the patch (L_p, W_p), feed line (L_{fi}, W_f) and ground $(L_g = L_s, W_g = W_s)$ are all optimized by using Sequential Quadratic Programing (SQP) algorithm which is one of the most successful method for nonlinear constrained optimization problems. Definition of all design parameters are given in Table 1. Since the aim of the study is to examine performance of the RMA at mm-wave band for various dielectric substrates and thicknesses, the most commonly used 5 dielectric materials are chosen for analysis and their specifications are summarized in Table 2.

Table 1. Design parameters of the RMA

Parameter	Definition
$L_s = L_g$	Substrate and ground patch length
$W_s = W_g$	Substrate and ground patch width
L_p	Upper patch length
W_p	Upper patch width
L_{fi}	Embedding distance of the inset feed
W_f	Width of the feed line
g	Gap between feed line and patch
h	Substrate thickness
t	Upper and ground patch thickness

Table 2. Specifications of dielectric materials used in analyses

Dielectric Substrate	Dielectric Constant	Tangent Factor
Rogers RT5880	2.2	0.0009
Rogers RO3003	3	0.0013
FR4 epoxy	4.4	0.02
Rogers RT6006	6.15	0.0019
Rogers RT6010	10.2	0.0023

To evaluate the impact of the substrate permittivity five test groups are established for dielectric materials listed in Table 2. Then, for each test group, multiple substrate thicknesses—specifically, 1.57 mm, 0.787 mm, 0.508 mm, 0.256 mm, and 0.125 mm— are utilized and analyzed in the test cases. This approach provides valuable insights into the effects of substrate height and permittivity on key antenna performance parameters, such as resonance frequency (f_r), return loss (S_{11}), gain (G), bandwidth (BW) and directivity by interpreting the results of the analyses.

The bandwidths (BW) of the designed antennas are calculated by the difference between the lower (f_{c1}) and upper (f_{c2}) cutoff frequencies, which correspond to a -10 dB return loss, within a continuous frequency spectrum. This criterion is widely recognized in mobile communication and, as such, is considered appropriate for practical applications. Additionally, in HFSS simulations, antenna gain is presented in decibels (dB) rather than decibels relative to an isotropic radiator (dBi). It is crucial to note that HFSS inherently normalizes all gain values in reference to an isotropic antenna. Therefore, the gain values expressed in dB in HFSS simulations can be directly interpreted as dBi.

In the Test Group#1, Rogers RT5880 material with a dielectric constant of ε_r=2.2 and a loss tangent of tanδ= 0.0009 is employed as the substrate. Test Cases 1.1 through 1.5 examine range of substrate thicknesses, specifically 1.57 mm, 0.787 mm, 0.508 mm, 0.256 mm, and 0.125 mm. The patch and feed line dimensions are optimized to achieve minimal return loss, alongside maximum gain and bandwidth at the 38 GHz resonance frequency. A comprehensive summary of all design and performance parameters for the simulated antennas is

provided in Table 3. Additionally, comparative return loss graphs for each substrate thickness are presented in Fig. 4. The far-field gain and 3D directivity patterns for this test group are visually represented in the supplementary document, Appendix 1, Fig. A1 (a) through (e), corresponding to the different substrate thicknesses: 1.57 mm, 0.787 mm, 0.508 mm, 0.256 mm, and 0.125 mm. In the gain patterns, $\emptyset = 0°$ and $\emptyset = 90°$ represents E and H-planes, with the indicated markers representing the main lobe magnitude at 38 GHz.

Similarly, in Test Group#2, all design cases are constructed by using substrate material Rogers RO3003 with a dielectric constant of ε_r=3 and a loss tangent of tanδ= 0.0013. After optimization and analyses are performed, Table 4 provides a comprehensive summary of all design and performance parameters for this test group. For visual representation of the performance parameters given in the table, far-field gain and 3D directivity patterns are represented in Fig. A2 (a) through (e), for substrate thicknesses defined previously. Also, comparative evaluation of return losses for each substrate thickness is given in Fig. A3. Both Fig. A2 and A3 can be found in the supplementary document, Appendix 1.

In Test Group#3, all design cases utilize FR4 epoxy substrate, characterized by a dielectric constant of ε_r=4.4 and a loss tangent of tanδ=0.02. Following optimization and analysis, Table 5 presents a comprehensive summary of all design and performance parameters for this group. For visual representation of the analyses results given in the table, far-field gain and 3D directivity patterns are presented in Fig. A4, panels (a) through (e), corresponding to the previously defined substrate thicknesses. Fig. A5 provides a comparative evaluation of return losses for each substrate thickness. Both Fig. A4 and A5 can be found in the supplementary document, Appendix 1.

In Test Group#4, all design cases employ Rogers RT6006 substrate, which has a dielectric constant of ε_r=6.15 and a loss tangent of tanδ=0.0019. Following optimization and analysis, Table 6 presents a comprehensive summary of all design and performance parameters for this test group. For visual representation of the analyses results given in the table, far-field gain and 3D directivity plots are shown in Fig. A6, (a) through (e), corresponding to the substrate thicknesses. Fig.A7 presents a comparative evaluation of return losses for each substrate thickness. Both Fig. A6 and A7 can be found in the supplementary document, Appendix 1.

Finally, In Test Group#5, Rogers RT6010 dielectric material characterized by a dielectric constant of ε_r=10.2 and a loss tangent of tanδ=0.0023 has been used as substrate for all design cases. Following optimization and analysis, Table 7 offers a comprehensive summary of all design and performance parameters for this test group. For visual representation of the analyses results

given in the table, far-field gain and 3D directivity patterns are presented in Fig. A8, from (a) to (e), corresponding to the substrate thicknesses. Fig. A9 provides a comparative evaluation of return losses for each substrate thickness. Both Fig. A8 and A9 can be found in the supplementary document, Appendix 1.

3. Results and Discussion

To assess the impact of substrate dielectric constant and thickness on antenna performance for the simulated design cases, the performance parameters are presented in Fig.4, Fig. A1 through A9 (see supplementary document, Appendix 1) and summarized in Tables 3 through 7 are compared. In Fig. 5. directivities, in Fig. 6 gains and in Fig. 7 band widths of designed antennas are plotted across various substrate thicknesses. In these figures, each colored line represents a test group with a specific dielectric constant. Finally, the key findings of this study are summarized as follows;

- First of all, the optimal thickness of the substrate is typically determined based on the wavelength within the dielectric material to facilitate ease of calculation and to prevent convergence issues in numerical simulations. For an operation frequency of 38 GHz, the wavelength in the free space is approximately 7.89 mm. The wavelength within the dielectric is estimated by dividing this value by the square root of the dielectric constant, resulting a wavelength of approximately 2.47 mm for the highest dielectric constant (ε_r=10.2) and 5.32 mm for the lowest dielectric constant (ε_r=2.2). In test case involving a very thick substrate with a thickness of h=1.57 mm, the ratio of the thickness to the wavelength within the dielectric material is around 0.635 for the ε_r=10.2. For high computational accuracy, this ratio is recommended to be below 0.1 [26]. As a result, to ensure convergence in the solution process, the number of iterations must be increased, which in turn leads to longer computational times especially for the thick substrate with high dielectric constant.

- One of the most well-known features of microstrip antennas is thick substrates with low dielectric constant provides wider bandwidth, and more loosely bound radiation field which increase antenna efficiency with the expanse of larger antenna size. Conversely, thin substrates with high permittivity confine the radiation mostly in the substrate, leading to more stable radiation due to tightly bounded fields which results in narrow bandwidth. These makes them less efficient but the advent of smaller antenna size. Similarly, general evolution of the study shows that decreasing substrate thicknesses also decrease bandwidth, for all test groups. The widest bandwidth which is 18.87 GHz was provided by the first test group with the dielectric constant of 2.2 and substrate thickness of 1.57 mm. However, except the

first test group, the widest bandwidth achieved for the thickness of 0.787 mm for all others (see Fig. 7). That means for most of the designs the optimum thickness for widest bandwidth should be around 0.787 mm. Although, the bandwidth of the antenna mainly depends on the dielectric constant, thickness and frequency, studies shows that dielectric losses also effective on the cut of frequencies and so the bandwidths [26]. On the other hand, the narrowest bandwidth values are provided by the simulations with thinner substrates (i.e. h=0.127 or 0.254 mm) and higher dielectric constant (i.e. ε_r=6.15 or 10.2), as expected.

- For the test groups utilizing substrates with higher dielectric constants (i.e. ε_r=6.15 or 10.2), the return loss graphs (see supplementary document, Appendix1, Fig. A7 and A9) reveal the occurrence of multiple resonance frequencies within the 25–50 GHz range. Additionally, these groups exhibit a significant limitation in terms of extremely narrow bandwidth. A very high dielectric constant substrate tightly confines the electromagnetic field within the material, leading to the excitation of multiple wave modes within a narrow frequency band, which results in multiple resonance peaks. Furthermore, substrates with high dielectric constants increase surface current, which enhances the interaction between radiating waves and surface waves, further contributing to the excitation of multiple resonant frequencies. These challenges are particularly critical for MIMO antenna arrays, as they may lead to mutual coupling, electromagnetic interference, and crosstalk effects.

- For the test groups using substrates with relatively low dielectric constants (i.e. ε_r=2.2, 3 or 4), thinner substrates result in higher gain, as seen from Fig. 6. This is because, for a thinner substrate where $L_p/h \gg 1$ or $W_p/h \gg 1$, the fringing field effect is reduced, indicating fewer losses. However, for these test groups, the optimal substrate thickness for maximizing gain is approximately 0.254 mm, which is not the minimum thickness used in analyses. When the substrate becomes excessively thin, the proximity of the patch to the ground plane increases the impact of conduction and dielectric losses. These losses cause energy dissipation within the substrate rather than allowing it to radiate effectively, leading to a decrease in overall antenna efficiency and gain. Therefore, while thinner substrates initially enhance gain by reducing losses and improving radiation efficiency, making the substrate excessively thin results in diminished radiation and increased losses, ultimately reducing the gain.

- In controversially, for the test group using substrates with the highest dielectric constants (ε_r=10.2), thinner substrates result in reduce gain (see Fig. 6).

The radiation mechanism in microstrip antennas controlled fringing fields at the edges of the patch. In high dielectric constant materials, fringing fields are weak and so, most of the electromagnetic energy is confined within the substrate material rather than radiated. As the substrate thickness decreases, the concentration of the electromagnetic field within the material increases, leading to greater energy absorption and consequently, lower radiation efficiency and reduced gain. This reduction in radiated energy also accounts for the very narrow bandwidths observed in this test group.

- Far-field gain and directivity patterns indicate that test groups utilizing thin substrates with relatively low dielectric constants (i.e. ε_r=2.2, 3 or 4) exhibit a significant concentration of radiated power directed almost perpendicularly to the antenna surface, with a very low tilt angle (see supplementary document, Appendix 1, from (a) through (e) in Fig. A1, A2 and A4). Additionally, for these test groups, the main lobe level is enhanced, while the back lobe level is diminished as the substrate thickness decreases. Conversely, test groups employing thin substrates with high dielectric constants (i.e. ε_r=6.15 or 10.2) demonstrate an almost bidirectional far-field radiation pattern (see supplementary document, Appendix 1, from (a) through (e) in Fig. A6 and A8).

- Among all test cases, the highest gain and directivity (~8.67 dB) is achieved by using the substrate RT5880 (ε_r=2.2) and a thickness of h=0.254 mm. However, the bandwidth for this test case is very narrow, approximately 0.7 GHz. On the other hand, the highest bandwidth (~18.8 GHz) across all test cases is achieved with the design using the substrate RT5880 (ε_r=2.2) and a thickness of h=1.57 mm. For this test case gain and directivity is around 5.9 dB (see Table 3 and Fig.5-7.)

- The test case with a substrate dielectric constant of ε_r=3 and a thickness of h=0.787 mm is particularly noteworthy due to its very wide bandwidth of approximately 17.6 GHz (46% of operation frequency) and relatively higher gain and directivity of around 7 dB, as given in Table 4. and Fig.5-7. This combination makes it a suitable choice for wide band antenna design with high efficiency.

- In contrast, for the test group utilizing a substrate with a very high dielectric constant (ε_r=10.2), the highest gain (7.9 dB) and directivity (8.3 dB) are achieved with thickest substrate (i.e. h=1.57mm). However, despite the high values of gain and directivity, bandwidth remains exceptionally narrow, ranging from 0.3 to 2.6 GHz across all substrate thicknesses (see Table 7 and Fig. 5–7). The use of a high-dielectric-constant substrate induces the excitation of multiple wave modes within a narrow frequency band and increases surface waves, which enhances the interaction between radiating waves and surface waves. This interaction reduces antenna efficiency and is particularly problematic for closely spacing array designs due to mutual coupling and crosstalk effects.

4. Conclusion

The objective of this study was to investigate the impact of key substrate properties on the performance of rectangular microstrip antennas (RMA), which is the most fundamental forms of microstrip antennas. The RMA was designed to operate at 38 GHz, targeting high-frequency 5G applications due to the low atmospheric attenuation in the Ka-band and simulations conducted over the frequency range of 25–50 GHz. To perform analyses, five test groups were established using well-known dielectric substrates, including RT5880, RO3003, FR4, RT6006, and RT6010. For each test group multiple substrate thicknesses (1.57 mm, 0.787 mm, 0.508 mm, 0.256 mm, and 0.125 mm) were utilized and analyzed in the design test cases to examine the effect of these variations on key antenna performance metrics, including resonance frequency (f_r), return loss (S_{11}), gain (G), bandwidth (BW) and directivity.

The findings of this study effectively demonstrate the relationship between substrate characteristics and antenna performance. The results indicate that selecting a substrate material with a lower dielectric constant (e.g., ε_r=2.2, 3 or 4) is critical for efficient millimeter-wave band RMA designs. Notably, the test case with a substrate dielectric constant of ε_r=3 and a thickness of h=0.787 mm stands out due to its exceptionally wide bandwidth of approximately 17.6 GHz (46% of the operating frequency) and relatively high gain and directivity, both around 7 dB. This combination makes it an ideal candidate for wideband antenna design with high efficiency in the millimeter-wave band.

In general, for low dielectric substrates, a trade-off between wider bandwidth and lower gain can be achieved by adjusting the substrate thickness and optimizing the antenna's size parameters. This flexibility allows the design to be tailored to specific applications, depending on the primary performance requirements. Conversely, substrates with very high dielectric constants (e.g., ε_r=10.2) leading to increased surface wave propagation, multiple resonant frequencies, and higher dielectric losses. These challenges are particularly significant for MIMO antenna arrays, where they can contribute to mutual coupling and crosstalk effects.

Overall, the results of this study provide valuable insights into the influence of substrate properties on RMA performance, offering guidance that can inform more advanced antenna design studies, particularly in the context of high-frequency 5G applications.

Table 3. Summary of all design and performance parameters for test cases in Test Group#1

	Parameter	Unit	Test Case 1.1	Test Case1.2	Test Case 1.3	Test Case 1.4	Test Case 1.5
	TEST GROUP #1 Dielectric Substrate: Rogers RT/duroid 5880 ($\varepsilon_r = 2.2, \tan\delta = 0.0009$)						
Design Parameters	h	mm	1.57	0.787	0.508	0.254	0.127
	$L_s = L_g$		8	7	6	6	6
	$W_s = W_g$		6	6	7	8	9
	L_p	mm	2.2978	1.835	2.157	2.4063	2.583
	W_p		3.852	3.913	3.33	3.336	2.9879
	L_{fi}		0.507	0.826	0.673	0.671	0.7534
	W_f		2.679	1.284	1.306	1.243	1.370
	g		0.199	0.1699	0.1048	0.116	0.1199
Performance Parameters	f_r	GHz	37.98	38.02	38.12	38.1	38.00
	$S11$	dB	-27.52	-30.36	-30.92	-37.33	-45.75
	$f_{c1} - f_{c2}$	GHz	25.54- 44.6	34.45-41.83	36.44-39.56	37.24-38.78	37.60-38.32
	BW	GHz	18.87	7.38	3.12	1.54	0.72
	G	dB	5.87	7.61	8.26	8.67	8.59
	$Directivity$	dB	5.89	7.53	8.23	8.67	8.67
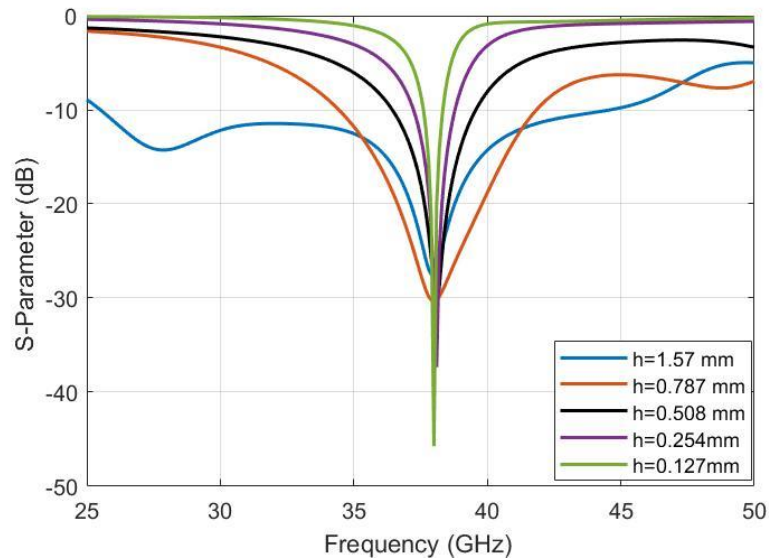
Figure 4. Comparison of Return loss (S11) graphs for Test Group#1 ($\varepsilon_r = 2.2$) across various thicknesses

Table 4. Summary of all design and performance parameters for test cases in Test Group#2

	Parameter	Unit	Test Case 2.1	Test Case 2.2	Test Case 2.3	Test Case 2.4	Test Case 2.5
	TEST GROUP #2 Dielectric Substrate: Rogers RO3003 ($\varepsilon_r = 3, \tan\delta = 0.0013$)						
Design Parameters	h	mm	1.57	0.787	0.508	0.254	0.127
	$L_s = L_g$	mm	6	6	6	6	6
	$W_s = W_g$		5.22	5.5	7	8	9
	L_p		1.218	1.535	1.832	2.2	2.321
	W_p		3.626	3.5	3.474	3.03	3
	L_{fi}		0.2925	0.28	0.388	0.302	0.5164
	W_f		1.942	1.76	1.693	1.913	1.694
	g		0.1	0.1	0.116	0.171	0.13
Performance Parameters	f_r	GHz	38.02	38.04	38.0	37.9	37.9
	$S11$	dB	-39.76	-43.91	-37.89	-43.78	-27.27
	$f_{c1} - f_{c2}$	GHz	28.26-39.63	34.23-51.87	36.12-39.56	36.82-38.72	37.57-38.18
	BW	GHz	11.37	17.64	3.44	1.9	0.6
	G	dB	5.84	7.11	7.62	8.16	7.81
	$Directivity$	dB	5.83	7.09	7.60	8.18	8.00

Table 5. Summary of all design and performance parameters for test cases in Test Group#3

	Parameter	Unit	Test Case 3.1	Test Case 3.2	Test Case 3.3	Test Case 3.4	Test Case 3.5
	TEST GROUP #3 Dielectric Substrate: FR4_epoxy ($\varepsilon_r = 4.4, \tan\delta = 0.02$)						
Design Parameters	h	mm	1.57	0.787	0.508	0.254	0.127
	$L_s = L_g$	mm	5.32	5	4	4.5	5
	$W_s = W_g$		3.56	4	5	6	7
	L_p		1.215	1.22	1.437	1.6849	1.9598
	W_p		3.23	2.92	3.0537	3.157	2.6728
	L_{fi}		0.27	0.25	0.25	0.2987	0.294
	W_f		1.87	1.5	1.2752	1.442	1.85
	g		0.1	0.1	0.05	0.078	0.086
Performance Parameters	f_r	GHz	38.0	38.08	37.92	38.14	38.0
	$S11$	dB	-40.46	-43.05	-35.80	-40.40	-43.05
	$f_{c1} - f_{c2}$	GHz	34.23-40.91	33.84-47.35	35.25-40.71	36.81-39.35	37.26-38.91
	BW	GHz	6.68	13.51	5.46	2.54	1.64
	G	dB	4.38	5.12	6.58	6.59	5.93
	$Directivity$	dB	5.08	5.64	7.15	6.59	7.96

Table 6. Summary of all design and performance parameters for test cases in Test Group#4

	Parameter	Unit	Test Case 4.1	Test Case 4.2	Test Case 4.3	Test Case 4.4	Test Case 4.5
	TEST GROUP #4 Dielectric Substrate: Rogers RT/duroid 6006 ($\varepsilon_r = 6.15, \tan\delta = 0.0019$)						
Design Parameters	h	mm	1.57	0.787	0.508	0.254	0.127
	$L_s = L_g$	mm	7.55	7	7.6	7	7
	$W_s = W_g$		5	5	5	5	5
	L_p		2.997	2.6954	2.74	3.043	3.1825
	W_p		3	2.114	3.43	2.6	2.107
	L_{fi}		0.5	0.3118	0.5	0.2634	0.3936
	W_f		1.877	1.275	1.4	1.0505	0.5
	g		0.1	0.0781	0.1	0.05	0.05
Performance Parameters	f_r	GHz	38.00	38.04	37.9	38.0	38.02
	$S11$	dB	-24.33	-31.47	-37.84	-29.23	-17.13
	$f_{c1} - f_{c2}$	GHz	37.45-38.55	35.39-40.07	37.23-38.52	37.78-38.24	37.93-38.11
	BW	GHz	1.1	4.68	1.29	0.46	0.18
	G	dB	6.16	6.12	6.31	6.40	6.00
	$Directivity$	dB	6.37	6.16	6.47	6.74	6.84

Table 7. Summary of all design and performance parameters for test cases in Test Group#5

	Parameter	Unit	Test Case 5.1	Test Case 5.2	Test Case 5.3	Test Case 5.4	Test Case 5.5
	— TEST GRUP #5 Dielectric Substrate: Rogers RT/duroid 6010 ($\varepsilon_r = 10.2, \tan\delta = 0.0023$)						
Design Parameters	h	mm	1.57	0.787	0.508	0.254	0.127
	$L_s = L_g$		8	6.5	7	7	7
	$W_s = W_g$		5.3	5.5	5.5	8	8
	L_p	mm	2.5737	3.99	2.271	2.3172	2.01
	W_p		4.127	3.5	3.54	3.93542	4.4556
	L_{fi}		0.8975	1.096	0.8481	0.8051	1.2498
	W_f		1.7441	1.9928	1.2862	1.0157	1.9501
	g		0.126	0.083	0.06437	0.0903	0.0587
Performance Parameters	f_r	GHz	38.0	38.06	37.96	38.04	38.0
	$S11$	dB	-43.89	-22.96	-36.62	-24.09	-24.7
	$f_{c1} - f_{c2}$	GHz	37.61-39.06	36.85-39.46	37.34-38.59	37.87-38.20	37.83-38.26
	BW	GHz	1.45	2.61	1.25	0.33	0.43
	G	dB	7.95	7.72	7.11	6.99	5.88
	$Directivity$	dB	8.35	7.86	7.30	7.67	6.92
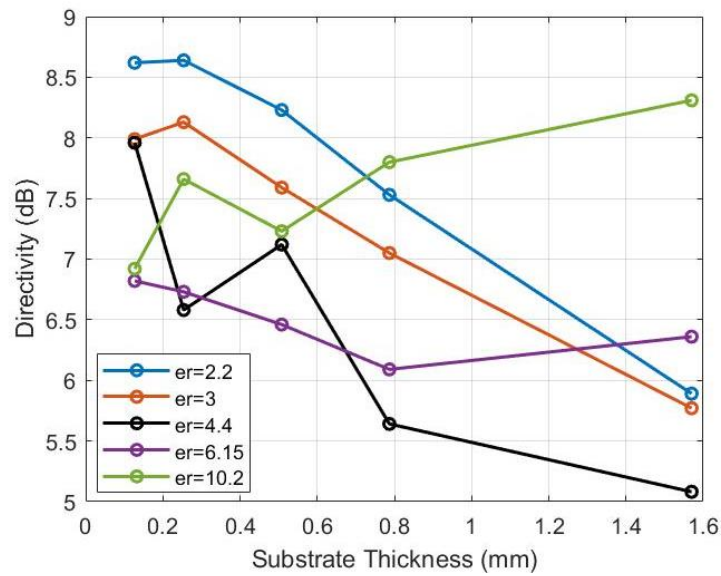
Figure 5. Comparison of directivities of designed antennas across various substrate thicknesses (each colored line represents a test group with a specific dielectric constant as indicated in the label)
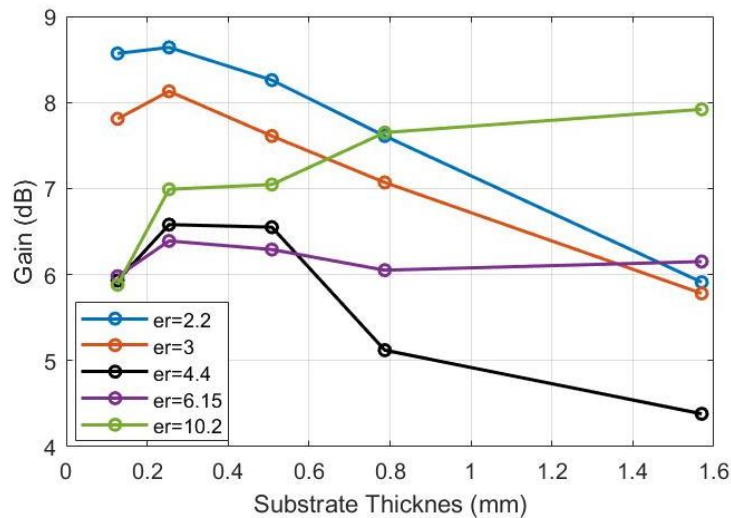
Figure 6. Comparison of gains of designed antennas across various substrate thicknesses (each colored line represents a test group with a specific dielectric constant as indicated in the label)
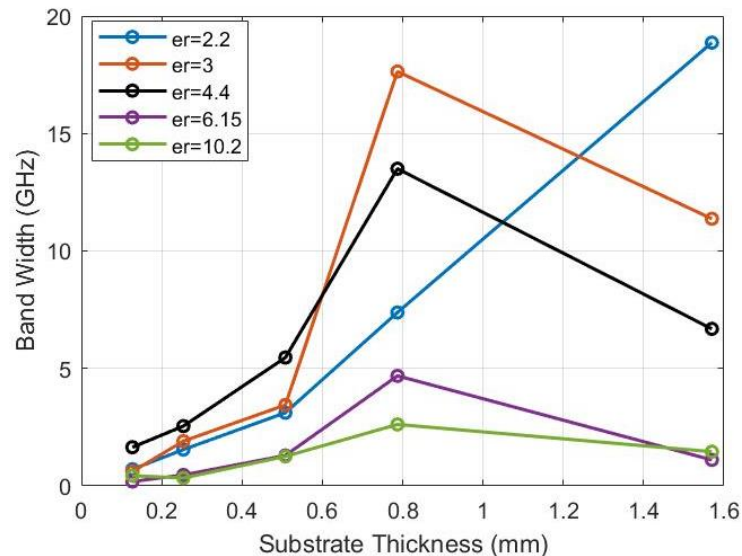
Figure 7. Comparison of band widths of designed antennas across various substrate thicknesses (each colored line represents a test group with a specific dielectric constant as indicated in the label)

References

[1]. Internet: Cisco "Visual Networking Index: Global Mobile Data Traffic Forecast Update, 2014–2019", 2015. Available: www.Cisco.com.

[2]. Internet: Cisco, "Global 2016 Year in Review", 2016. Available: www.Cisco.com.

[3]. Agiwal, M., Roy, A., & Saxena, N. 2016. Next generation 5G wireless networks: A comprehensive survey. *IEEE Communications Surveys & Tutorials*, 18(3), 1617-1655.

[4]. Yang, Y., Xu, J., Shi, G., & Wang, C. X. 5G Wireless Systems. Springer International Publishing, 2018; pp 2-7.

[5]. Demirci M., 5G Haberleşme Teknolojisi için Mikroşerit Yama Anten Tasarımı, Master's Thesis, Osmaniye Korkut Ata Üniversitesi, Osmaniye, 2020.

[6]. Internet: Aselsan, "Yeni Nesil Geniş Bantlı Haberleşme Teknolojileri, 5G Nedir?", ISSN 1300-2473, 35(111), 2022; pp 26-30. Available: www.aselsan.com.tr

[7]. Parchin, N. O., Mohamed, H. G., Moussa, K. H., See, C. H., Abd-Alhameed, R. A., Alwadai, N. M., & Amar, A. S. 2023. An efficient antenna system with improved radiation for multi-standard/multi-mode 5G cellular communications. *Scientific Reports,* 13(1), 4179.

[8]. Raj, T., Mishra, R., Kumar, P., & Kapoor, A. 2023. Advances in MIMO antenna design for 5G: A comprehensive review. *Sensors,* 23(14), 6329.

[9]. Krishnamoorthy, R., Kumar, U. S., Swathi, G., Begum, M. A., Nancharaiah, B., & Sagar, K. D. 2023. Metamaterial inspired quad-port multi-antenna system for millimeter wave 5G applications. *Journal of Infrared, Millimeter, and Terahertz Waves,* 44(5), 346-364.

[10]. Al-Azzawi, Z. F., AbdulSattar, R. K., Muhsin, M. Y., Azeez, M. A., Salim, A. J., & Ali, J. K. 2023. Designing eight-port antenna array for multi-band MIMO applications in 5G smartphones. *Journal of Telecommunications and Information Technology*, (4).

[11]. Chbeine, M., Azmani, M., & Astito, A. Advanced UWB MIMO Antenna with Wide Bandwidth and High-Efficiency Performance for 5G. 11th International Conference on Signal Processing and Integrated Networks (SPIN), IEEE. 2024, March, pp. 227-232.

[12]. Ibrahim, S. K., Singh, M. J., Al-Bawri, S. S., Ibrahim, H. H., Islam, M. T., Islam, M. S. & Abdulkawi, W. M. 2023. Design, challenges and developments for 5G massive MIMO antenna systems at sub 6-GHz band: a review. *Nanomaterials,* 13(3), 520.

[13]. Cao, T. N., Nguyen, M. T., Phan, H. L., Nguyen, D. D., Vu, D. L., Nguyen, T. Q. H., & Kim, J. M. 2023. Millimeter-wave broadband MIMO antenna using metasurfaces for 5G cellular networks. *International Journal of RF and Microwave Computer-Aided Engineering*, 2023(1), Article ID 9938824. https://doi.org/10.1155/2023/9938824

[14]. Sharaf, M. H., Zaki, A. I., Hamad, R. K., & Omar, M. M. (2020). A novel dual-band (38/60 GHz) patch antenna for 5G mobile handsets. *Sensors,* 20(9), 2541.

[15]. Demirci, M., Ermiş, S. 2021. 5G teknolojisi için çift bantlı (28/38 GHz) dikdörtgen mikroşerit anten tasarımı. *Bilişim Teknolojileri Dergisi*, 14(2), 171-181.

[16]. Haneef, S. R., Selvaperumal, S. K., & Jayapal, V. 2020. High gain rectangular single patch antenna at mmwave band. In*ternational Journal of Advanced Science and Technology,* 29(1), pp. 1311- 1325.

[17]. Ramli, N., Noor, S. K., Khalifa, T., & Abd Rahman, N. H. 2020. Design and performance analysis of different dielectric substrate based microstrip patch antenna for 5G applications. *International Journal of Advanced Computer Science and Applications*, *11*(8).

[18]. Ahmad, I., Sun, H., Zhang Y. & Samad, A. High Gain Rectangular Slot Microstrip Patch Antenna for 5G mm-Wave Wireless Communication, 5th International Conference on Computer and Communication Systems (ICCCS), Shanghai, China, 2020, pp. 723-727, doi: 10.1109/ICCCS49078.2020.9118602.

[19]. Sree, M. F. A., Abd Elazeem, M. H., & Swelam, W. Dual Band Patch Antenna Based on Letter Slotted DGS for 5G Sub-6GHz Application. In Journal of Physics: Conference Series, IOP Publishing, Vol. 2128, No. 1, 2021, December, p. 012008.

[20]. Marasco, I., Niro, G., Mastronardi, V. M., Rizzi, F., D'Orazio, A., De Vittorio, M., & Grande, M. 2022. A compact evolved antenna for 5G communications. *Scientific reports,* 12(1), 10327.

[21]. Yadav, J., Sharma, S., & Arora, M. 2022. A paper on microstrip patch antenna for 5G applications. *Materials Today: Proceedings*, *66*, 3430-3437.

[22]. Ermiş, S., & Demirci, M. 2023. Improving the performance of patch antenna by applying bandwidth enhancement techniques for 5G applications. *Tehnički glasnik*, 17(3), 305-312.

[23]. Kumar, L., Nath, V., & Reddy, B. V. R. 2023. Triple-band stub loaded patch antenna with high gain for 5G Sub-6 GHz, WLAN and WIMAX applications using DGS. *Facta Universitatis, Series: Electronics and Energetics*, 36(2), 171-188.

[24]. Es-saleh, A., Bendaoued, M., Lakrit, S., Das, S., Atounti, M., & Faize, A. 2023. A novel fractal patch antenna using Defected Ground Structure (DGS) with high isolation for 5G applications. Journal of Nano- and Electronic Physics, 15(3), 03012(4pp).

[25]. Balanis, C. A. Antenna Theory: Analysis and Design. Second Edition, John Wiley & Sons, 2016, pp 722-784.

[26]. Garg, R. Microstrip Antenna Design Handbook. Artech House, 2001, pp 253-314.

Appendix 1.
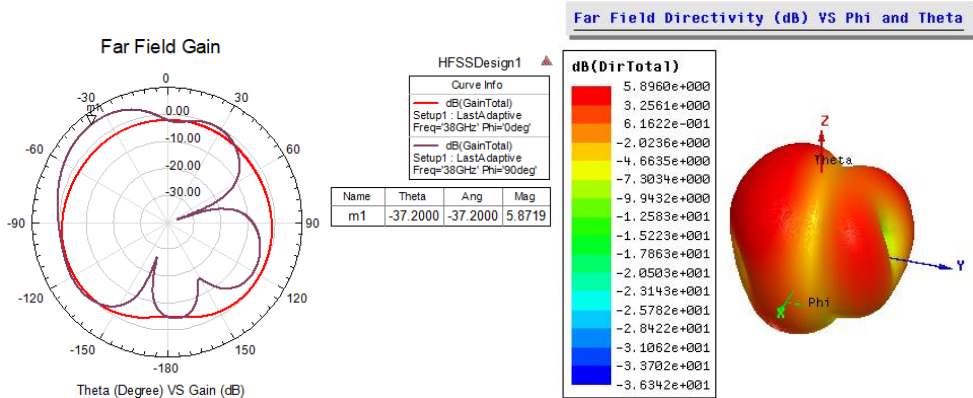
(a)
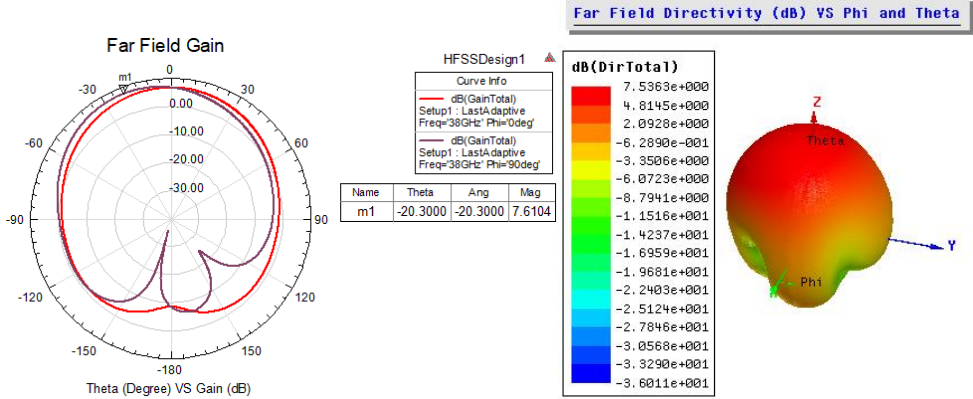
(b)
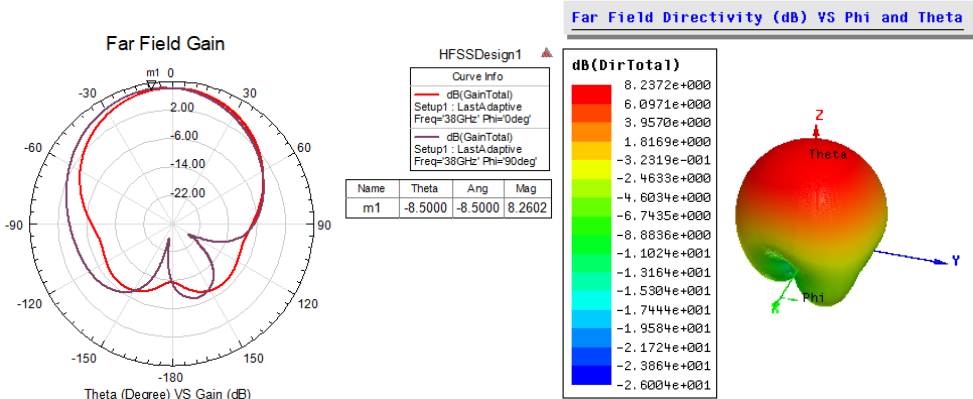
(c)
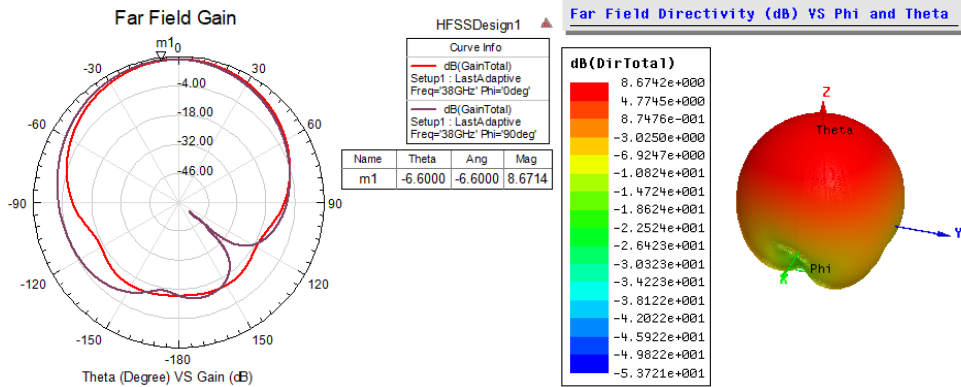
(d)
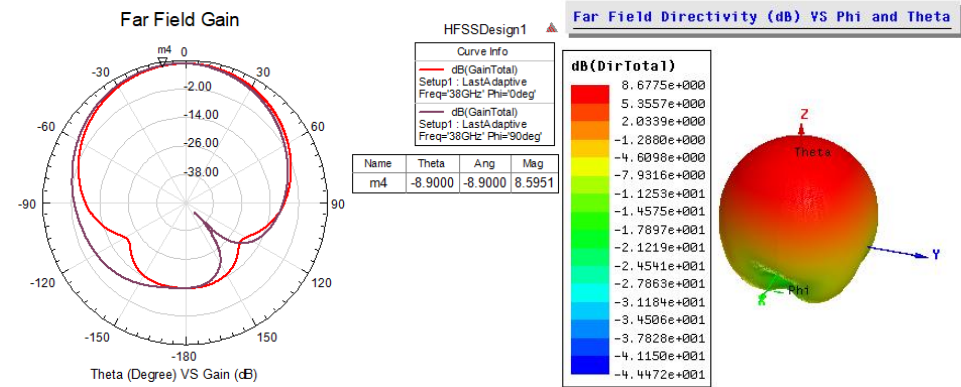
(e)

Figure A1. Far field gain and 3D directivity patterns for Test Group#1 ($\varepsilon_r = 2.2$) with varying substrate thicknesses; h=1.57mm **(a)**, h=0.787mm **(b)**, h=0.508mm **(c)**, h=0.254mm **(d)** and h=0.127 mm **(e)**
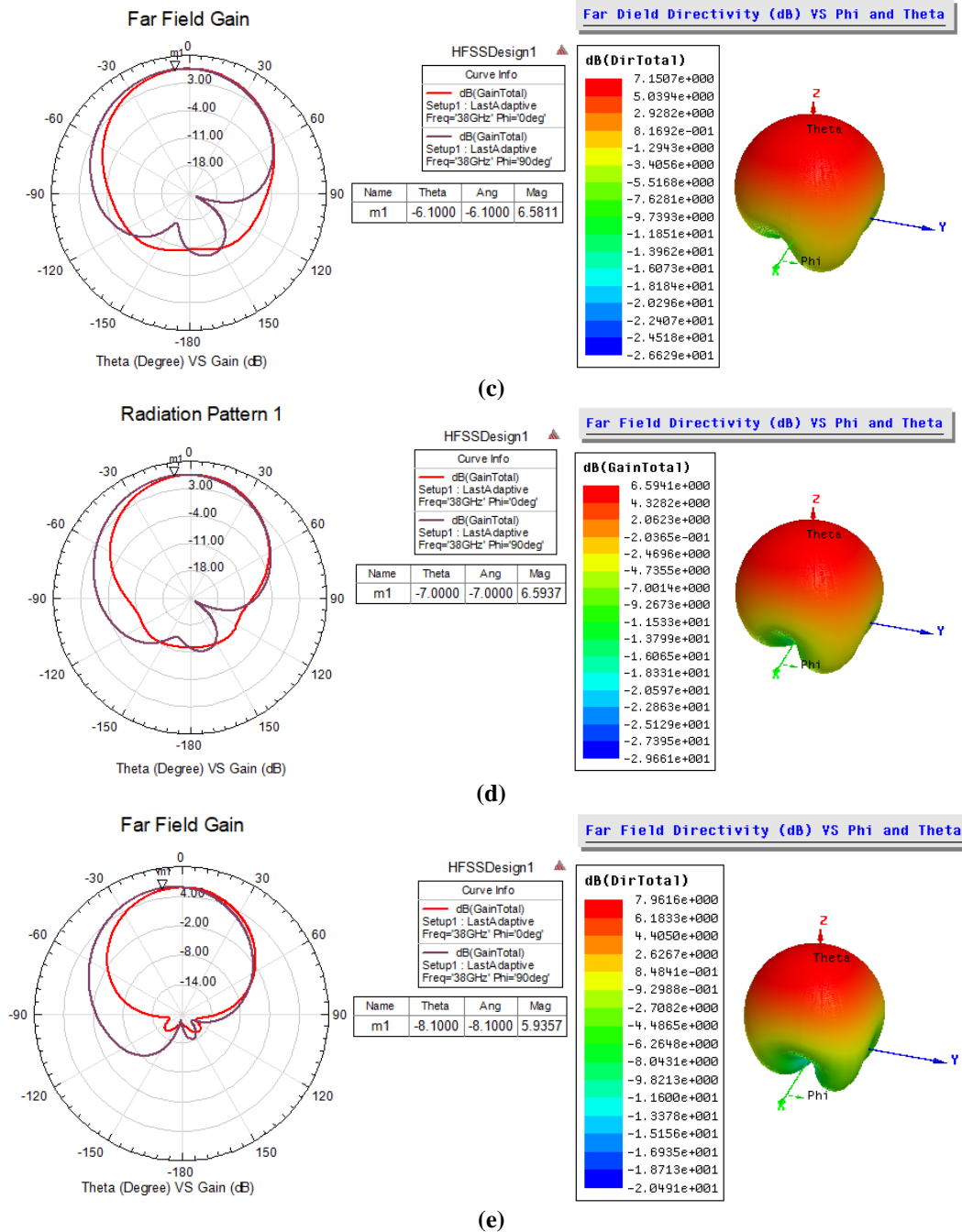

(a)

(b)

(c)

(d)

(e)
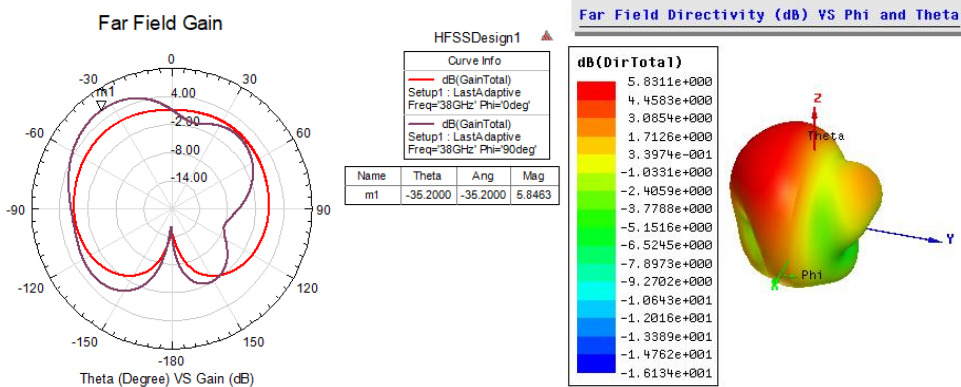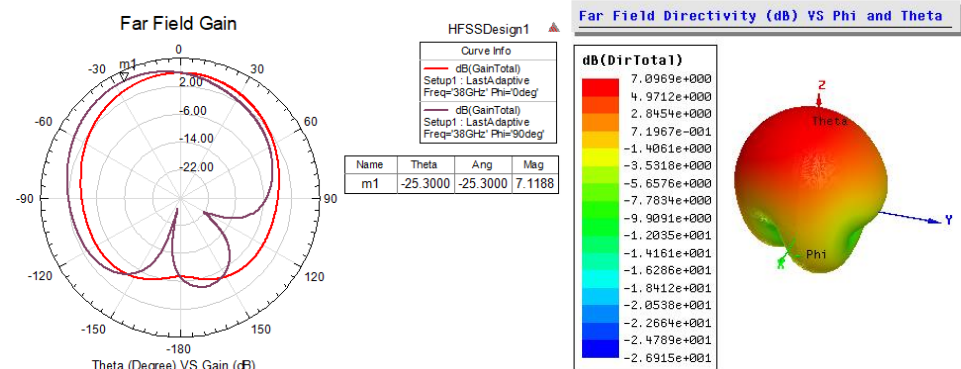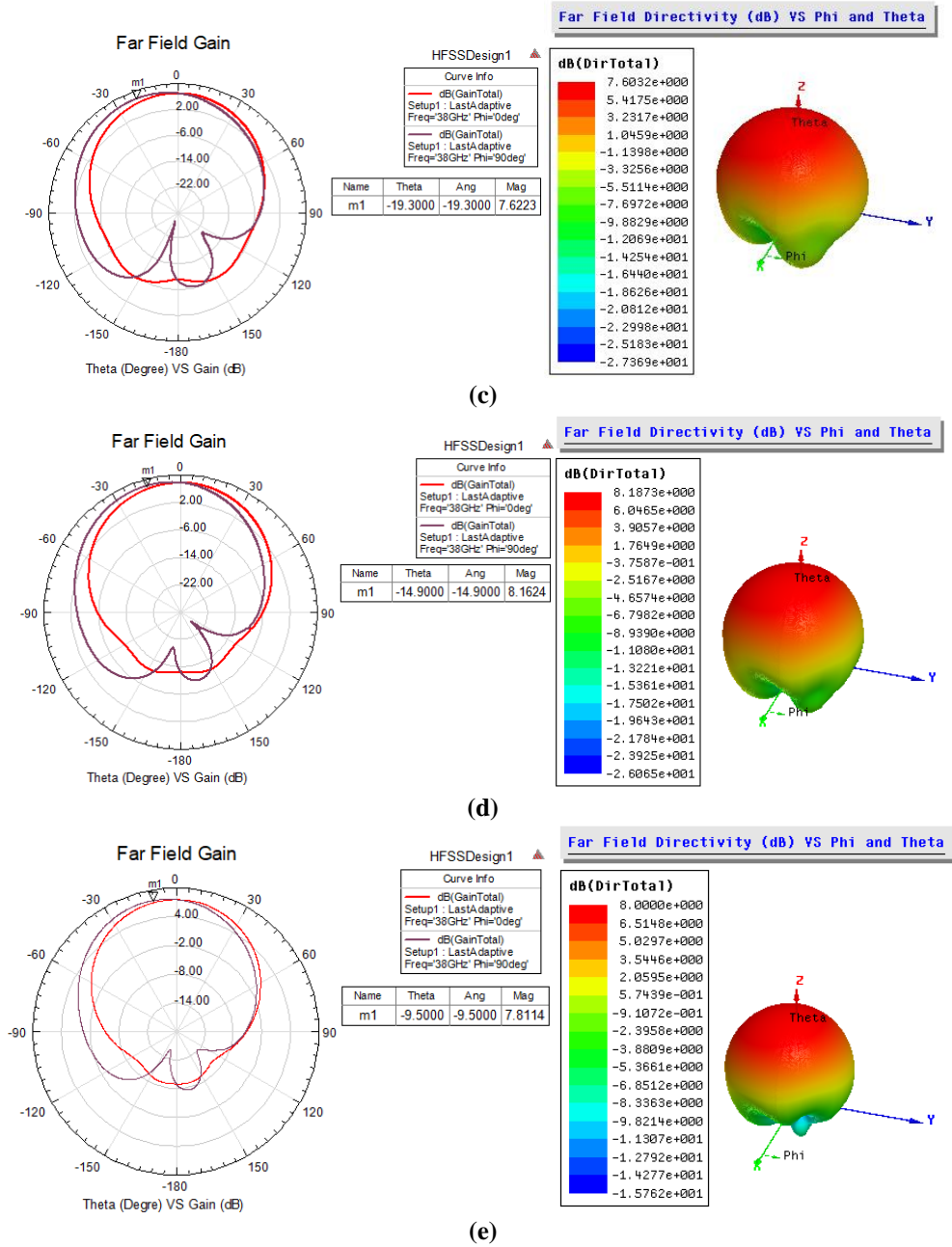
Figure A2. Far field gain and 3D directivity patterns for Test Group#2 ($\varepsilon_r = 3$) with varying substrate thicknesses; h=1.57mm **(a)**, h=0.787mm **(b)**, h=0.508mm **(c)**, h=0.254mm **(d)** and h=0.127 mm **(e)**
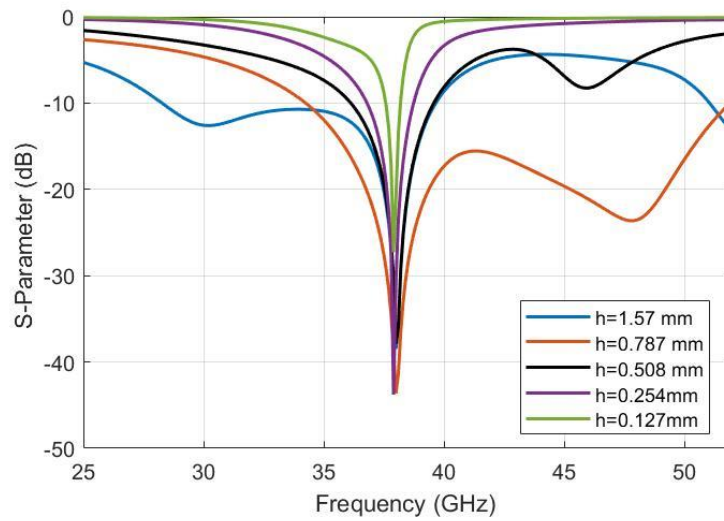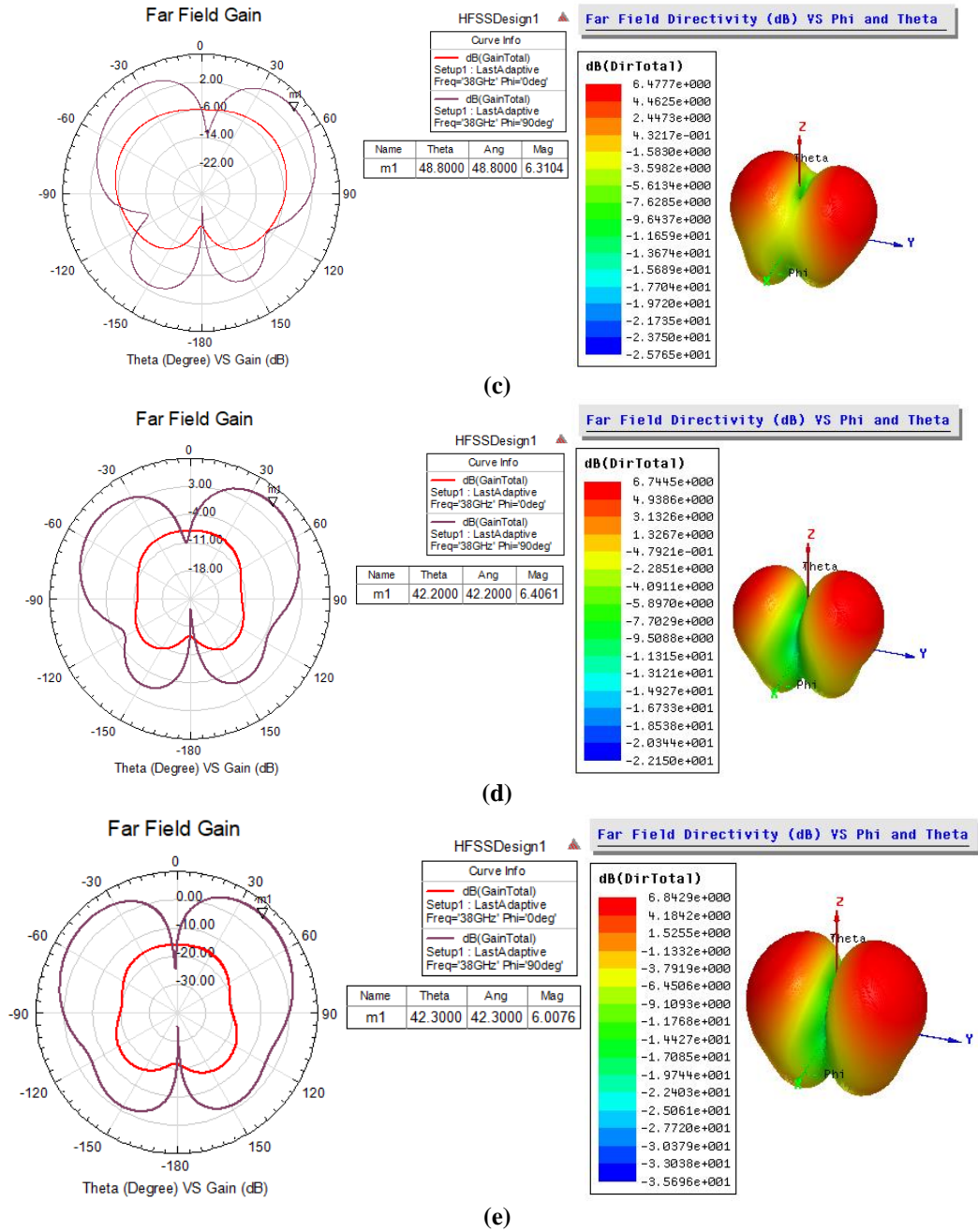
Figure A3. Comparison of Return loss (S11) graphs for Test Group#2 ($\varepsilon_r = 3$) across various thicknesses

(a)

(b)

S. Ermis

(c)

(d)

(e)
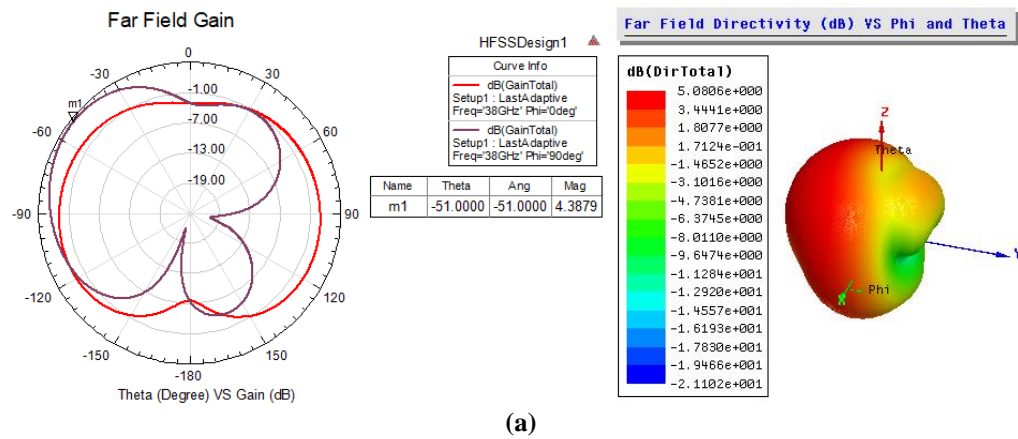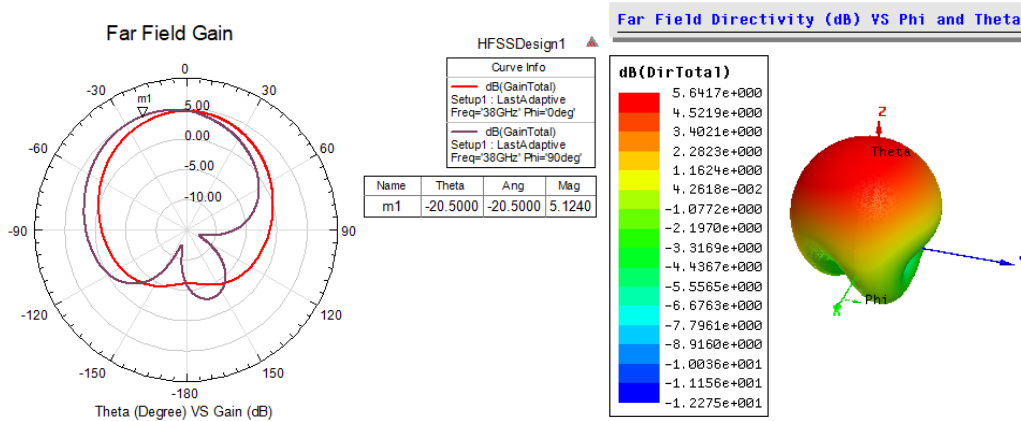
Figure A4. Far field gain and 3D directivity patterns for Test Group#3 ($\varepsilon_r = 4.4$) with varying substrate thicknesses; h=1.57mm **(a)**, h=0.787mm **(b)**, h=0.508mm **(c)**, h=0.254mm **(d)** and h=0.127 mm **(e)**
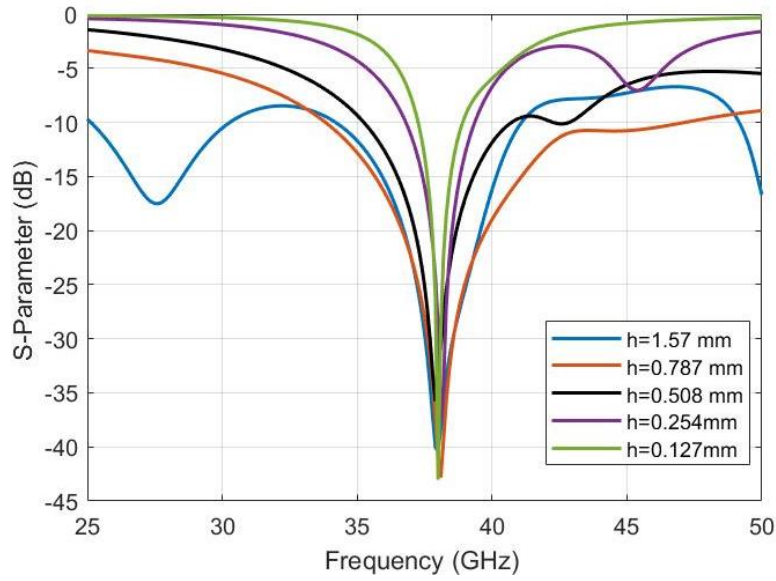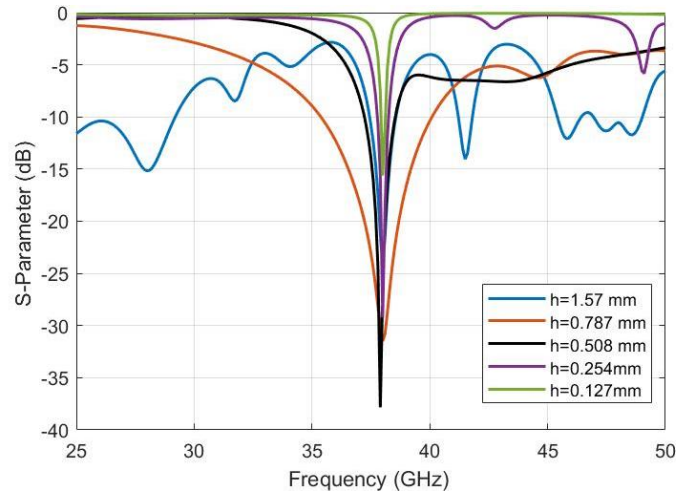
Figure A5. Comparison of Return loss (S11) graphs for Test Group#3 ($\varepsilon_r = 4.4$) across various thicknesses

(a)

(b)

S. Ermis

(c)

(d)

(e)
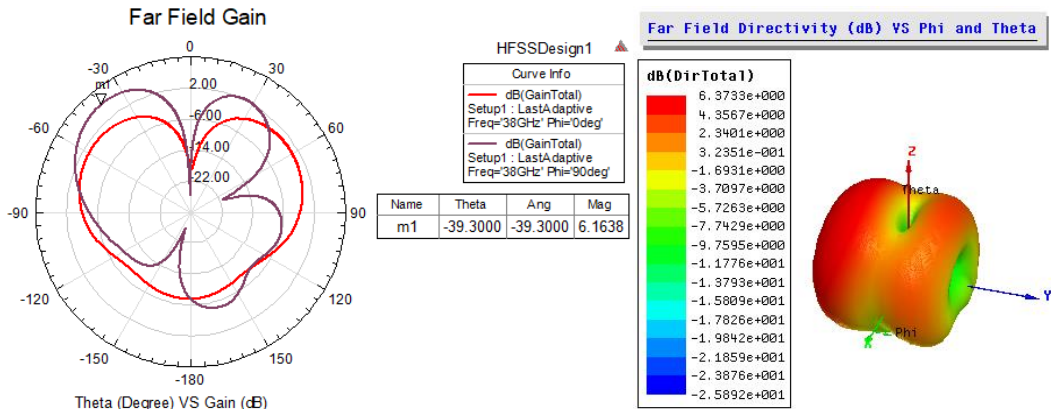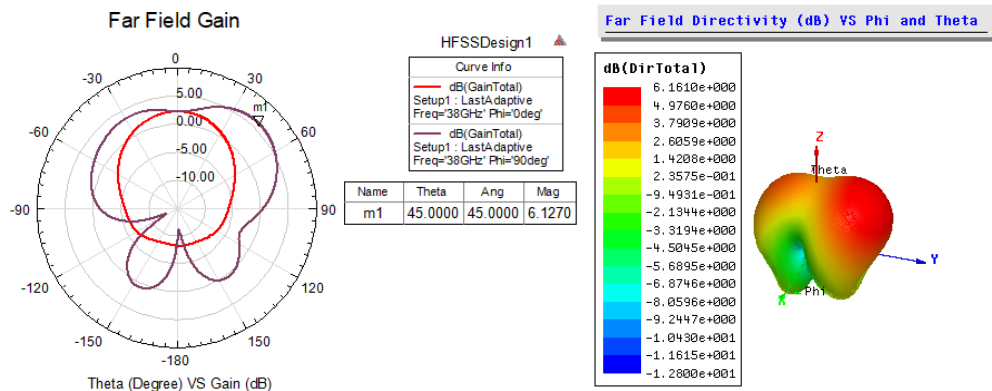
Figure A6. Far field gain and 3D directivity patterns for Test Group#4 ($\varepsilon_r = 6.15$) with varying substrate thicknesses; h=1.57mm **(a)**, h=0.787mm **(b)**, h=0.508mm **(c)**, h=0.254mm **(d)** and h=0.127 mm **(e)**
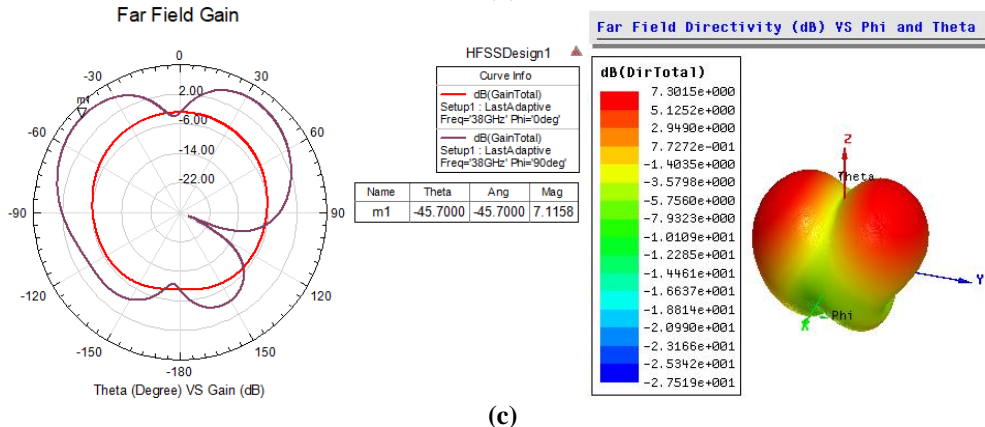
Figure A7. Comparison of Return loss (S11) graphs for Test Group#4 ($\varepsilon_r = 6.15$) across various thicknesses
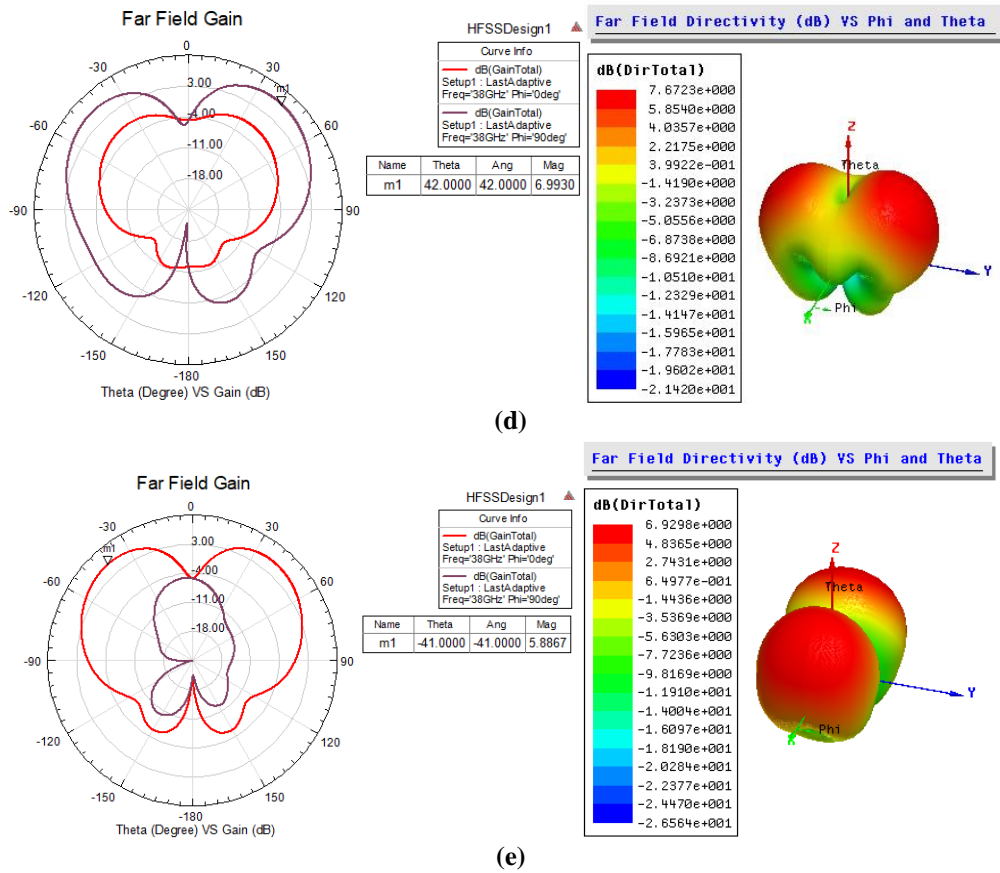

(a)

(b)

(c)

(d)

(e)
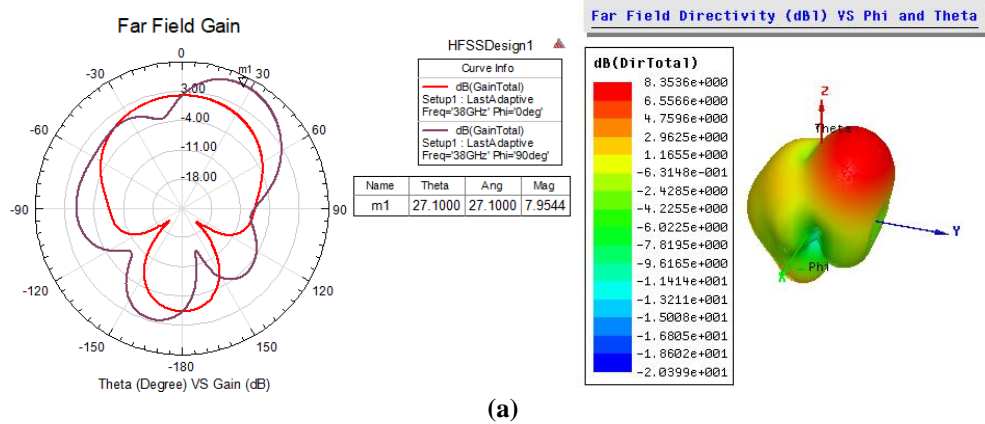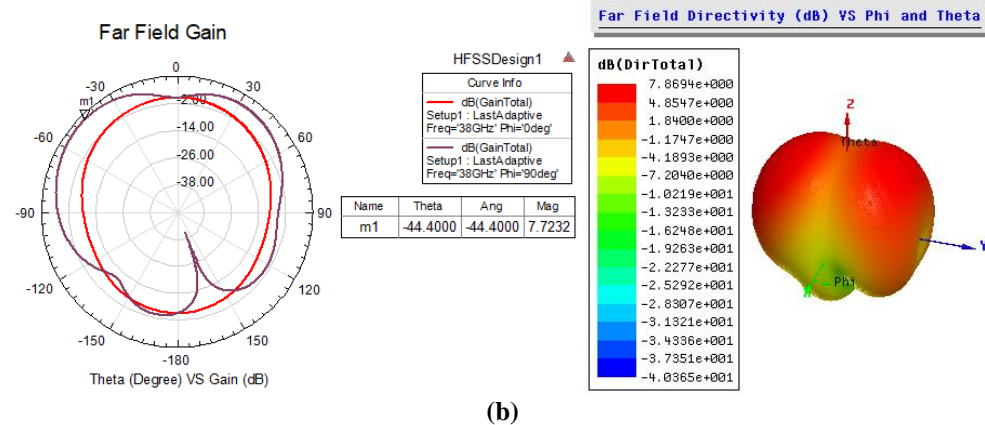
Figure A8. Far field gain and 3D directivity patterns for Test Group#5 ($\varepsilon_r = 10.2$) with varying substrate thicknesses; h=1.57mm **(a)**, h=0.787mm **(b)**, h=0.508mm **(c)**, h=0.254mm **(d)** and h=0.127 mm **(e)**

Figure A9. Comparison of Return loss (S11) graphs for Test Group#5 ($\varepsilon_r = 10.2$) across various thicknesses